

Elucidating the Structure of Surface Acid Sites on γ -Al₂O₃

Peter J. Chupas,* Karena W. Chapman,* and Gregory J. Halder

X-ray Science Division, Advanced Photon Source, Argonne National Laboratory, Argonne, Illinois 60439, United States

S Supporting Information

ABSTRACT: Differential pair distribution function analysis was applied to resolve, with crystallographic detail, the structure of catalytic sites on the surface of nanoscale γ -Al₂O₃. The structure was determined for a basic probe molecule, monomethylamine (MMA), bound at the minority Lewis acid sites. These active sites were found to be five-coordinate, forming distorted octahedra upon MMA binding. This approach could be applied to study the interaction of molecules at surfaces in dye-sensitized solar cells, nanoparticles, sensors, materials for waste remediation, and catalysts.

Solid acids find widespread industrial application as heterogeneous catalysts, including in hydrocarbon cracking and producing halocarbon-based refrigerants.^{1–3} However, direct determination of the structure of the active acidic surface sites remains elusive. The structural uncertainty derives from the inherent difficulty in differentiating minority surface sites from the bulk using standard spectroscopic and structural characterization tools. Conventional scattering probes of surface structure (e.g., crystal truncation rod or X-ray standing wave analysis) require single crystals. Many important acid catalysts cannot be prepared as single crystals. This is particularly true for transition or metastable forms of aluminas, widely used catalysts and catalyst supports, which include γ -Al₂O₃, the prototypical acid catalyst. The flexible alumina geometries tolerate a wide range of distortions and coordination numbers (four, five, six). Although, much has been inferred by studying model molecular analogues and crystalline zeolites, a direct experimental probe that recovers accurate distances and site geometries has not yet been realized. Previous studies investigating the nature of the Lewis acid sites on γ -Al₂O₃ have applied solid state NMR,⁴ vibrational spectroscopy (Raman and infrared),⁵ computational methods,⁶ temperature-programmed desorption,⁷ and electron microscopy.⁸ While these allow us to quantify the number and type of acid sites, the insights provide far from the crystallographic level of detail needed to predict and optimize reactivity.

By directly measuring atom–atom distances between a basic probe molecule and the surface, we unravel the geometry of the coordinately unsaturated Lewis acid site on the surface of γ -Al₂O₃ with crystallographic detail. We probe the surface structure using differential pair distribution function (d-PDF) measurements of monomethylamine (CH₃NH₂) bound to acid sites on γ -Al₂O₃. The d-PDF approach selectively recovers only the atom–atom distances involving the bound molecules: correlations within the MMA probe molecule and between the MMA and the surface.

High surface area (402 m² g⁻¹, see Supporting Information), γ -phase aluminum oxide was prepared via hydrolysis of aluminum ethoxide.⁹ The sample was loaded into a flow cell,^{10,11} dried in situ under helium at 673 K for 2 h, and immediately cooled to 80 K. Data suitable for PDF analysis were collected at the Advanced Photon Source at beamlines 1-ID-C and 11-ID-B. Data were obtained for the dehydrated sample in helium and after exposure to either MMA or N₂ gas. High-energy X-rays (\sim 77 keV, λ = 0.1612 Å; \sim 60 keV, λ = 0.2128 Å) were used in combination with an amorphous silicon-based area detector.¹² The PDFs, $G(r)$, were obtained from the X-ray scattering data as described previously.¹²

The bulk structure of the γ -Al₂O₃ was verified by refining a model against the PDF emulsion data for the nonloaded, dehydrated material (Figure 1). The structure consists of corner- and edge-shared Al octahedra and tetrahedra. A tetragonally distorted *c*-centered model and a cubic spinel model were tested.¹³ The tetragonal model provided a better fit to the data ($R_w \sim$ 27%); a fit of comparable quality to that reported for boehmite-derived γ -Al₂O₃.¹⁴ Features in the residual at short distances indicate that some local structure distortions are not fully described by this model. The absence of correlations beyond \sim 35 Å indicates that the γ -Al₂O₃ exists as nanoparticles of \sim 3.5 nm diameter.¹⁵ This is consistent with the high surface area of the sample.

The d-PDF was obtained by subtracting a reference PDF, collected for the dehydrated sample under He, from the PDF of the MMA-loaded sample (Figure 1). The d-PDF contains both intramolecular correlations within the MMA molecule and correlations arising from interaction of the MMA molecule and the γ -Al₂O₃ surface. Being a strong base (pK_a = 10.62), of strength similar to that of trimethylphosphine, MMA binds to all acid sites. MMA was selected as a probe molecule over a simpler molecule, such as ammonia, so that the intensity of the N–C correlation could be used as a reference to quantify the relative loading level. Larger probe molecules, such as trimethylphosphine, have more intramolecular correlations which would unnecessarily complicate the analysis.

Several well-defined correlations are evident in the d-PDF at low r . These occur at distances below 2.5 Å, centered at 1.09, 1.45, 2.00, and 2.38 Å. The MMA molecule has C/N–H distances of \sim 1.1 Å, and a C–N distance of \sim 1.48 Å.¹⁶ The presence of additional well-defined correlations not intrinsic to the probe molecule (2.00 Å, 2.38 Å) indicated that the MMA forms strong bonds to the surface acid sites. By contrast, d-PDFs for physisorbed gases are generally broad (Figure 1), with features at longer distances, as seen for N₂ within the nanopores of a Prussian blue analogue.¹⁷ Due to the low Z of the atoms involved, it would not be possible to gain these insights from an EXAFS experiment.

Received: April 8, 2011

Published: May 12, 2011

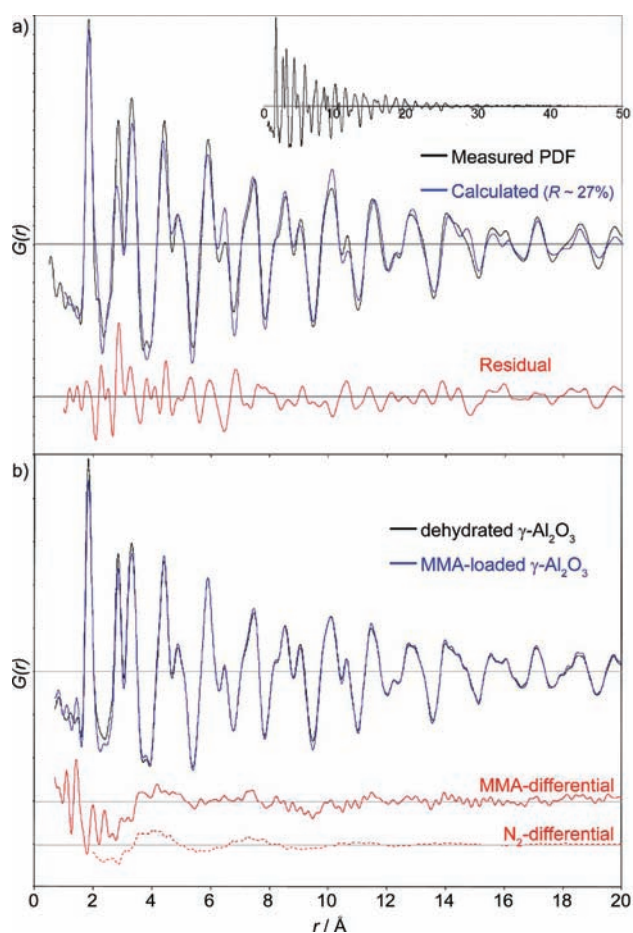


Figure 1. (a) PDF, $G(r)$, measured for $\gamma\text{-Al}_2\text{O}_3$, the calculated PDF for the best model fit to the data, and the residual to the fit. (b) d-PDF was obtained by subtracting a reference PDF collected for the dehydrated $\gamma\text{-Al}_2\text{O}_3$ from that measured for the MMA-loaded sample. The differential corresponding to physisorbed N_2 is given for reference.

The well-defined intermolecular correlations between the bound MMA and the $\gamma\text{-Al}_2\text{O}_3$ were tentatively assigned on the basis of relative distance. The shorter correlation (2.00 Å) was assigned to direct bonding of the amine at the Lewis acid site (N–Al). The longer correlation (2.38 Å) was assigned to the next-nearest neighbor distance between the amine and the Al-coordinated O atoms (N···O). d-PDFs were calculated for structural models based on these assignments. A model of MMA, based on the bond lengths indicated in the data, was treated as a rigid body, iteratively varying its distance and orientation relative to the surface. A model with four N···O correlations per MMA molecule yielded a significantly better fit to the data than one with only three N···O correlations. This indicated that Lewis acid sites are five-coordinate (AlO_5), and not four-coordinate, in the unreacted state, leading to a six-coordinate MMA-bound Al. The five-coordinate nature of the acid sites is consistent with solid state NMR studies of this system,⁹ where fluorination of the surface Al exclusively consumes the five-coordinate Al. Rotation of the MMA about the Al–N bond did not significantly impact the quality of the fit, suggesting that the MMA is free to precess about this bond. The N···O and N–Al distances in the d-PDF suggest a distortion of the Al octahedra, with the Al displaced below the plane of four O atoms by ~ 0.45 Å. The model and fit are shown in Figure 2.

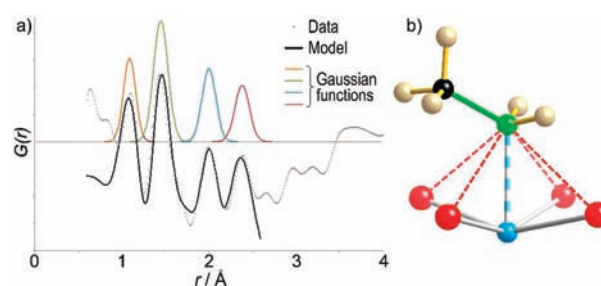


Figure 2. (a) Low r region of the d-PDF. The PDF calculated for the model of MMA-bound at the surface acid sites is shown in black. Atomic distances were estimated from Gaussian functions fit to well-defined features in the PDF. (b) The model of the bound-MMA. The bonds are colored to match the corresponding Gaussian peak.

The absence of sharp features in the d-PDF beyond 2.5 Å is consistent with increased disorder between the surface and the remote methyl group in the MMA. Specifically, the MMA molecule is free to rotate about the N–Al bond and forms no well-defined correlations with the $\gamma\text{-Al}_2\text{O}_3$. The broad feature at ~ 4 Å can be attributed to the distance between the dynamic methyl group and the $\gamma\text{-Al}_2\text{O}_3$ surface.

The Al–N bond length of 1.94 Å, found here for $\gamma\text{-Al}_2\text{O}_3$ -bound MMA, is within the range of distances reported for amine ligands coordinated to organometallic aluminum clusters (1.88–2.05 Å),^{18,19} molecular analogues used to understand Lewis acid sites in $\gamma\text{-Al}_2\text{O}_3$. However, most of these clusters involve tetrahedrally coordinated Al, a limitation of analyzing discrete molecular clusters to understand active surface sites. Only one example has an octahedral aluminum environment ($d_{\text{Al-N}} \approx 2.05$ Å).¹⁸

The data indicate that binding of MMA does not significantly perturb the surface structure. This is evidenced by the invariance of long distances in the PDF, which remain unchanged upon MMA binding. However, even if surface reorganization were evident, distortions of the AlO_x polyhedral would minimally impact the low r region of the d-PDF (< 2.5 Å) which contains the correlations characteristic of the bound MMA.

The application of d-PDF methods enabled us to identify the structure of the Lewis acid sites in $\gamma\text{-Al}_2\text{O}_3$, which are minority sites on the surface of nanosized particles. These acid sites account for 1 in 8 surface Al in such sol–gel derived $\gamma\text{-Al}_2\text{O}_3$ ⁹ or, for this system with $400 \text{ m}^2 \text{ g}^{-1}$ surface area, approximately 1 in 50 of all Al or ~ 1.6 wt % bound MMA. This surface structure analysis was only made possible using the differential approach; direct refinement of models for the MMA-loaded sample would be nearly impossible due to ambiguity in the model for the bulk $\gamma\text{-Al}_2\text{O}_3$, such that the contribution from the surface-bound MMA is smaller than the residual to the fit of the bulk phase. This analysis provides crystallography-like structural detail relating to binding at active surface sites. This level of structural resolution is needed to compare to real materials with computational simulations. This approach could be applied to other areas where the interaction of molecules at surfaces is important, such as dye-sensitized solar cells, nanoparticles, sensors, materials for waste remediation, and catalysts.

■ ASSOCIATED CONTENT

S Supporting Information. Details of the PDF and sorption analysis. This material is available free of charge via the Internet at <http://pubs.acs.org>.

AUTHOR INFORMATION**Corresponding Author**

chupas@aps.anl.gov; chapmank@aps.anl.gov

ACKNOWLEDGMENT

Work performed at Argonne National Laboratory was supported by the U.S. DOE, Office of Science, Office of Basic Energy Sciences, under Contract No. DE-AC02-06CH11357. C. P. Grey is thanked for useful discussions and P. L. Lee is thanked for instrument support.

REFERENCES

- (1) Knozinger, H.; Ratnasamy, P. *Catal. Rev. - Sci. Eng.* **1979**, *17*, 31–70.
- (2) Busca, G. *Chem. Rev.* **2007**, *107*, 5366–5410.
- (3) Manzer, L. E.; Rao, V. N. M. *Adv. Catal.* **1993**, *39*, 329–350.
- (4) Coster, D.; Blumenfeld, A. L.; Fripiat, J. J. *Phys. Chem.* **1994**, *98*, 6201–6211.
- (5) Liu, X. S.; Truitt, R. E. *J. Am. Chem. Soc.* **1997**, *119*, 9856–9860.
- (6) Sohlberg, K.; Pantelides, S. T.; Pennycook, S. J. *J. Am. Chem. Soc.* **2001**, *123*, 26–29.
- (7) Satsuma, A.; Kamiya, Y.; Westi, Y.; Hattori, T. *Appl. Catal., A.* **2000**, 253–263.
- (8) Kwak, J. H.; Hu, J. Z.; Mei, D.; Yi, C. W.; Kim, D. H.; Peden, C. H. F.; Allard, L. F.; Szanyi, J. *Science* **2009**, *325*, 1670–1673.
- (9) Chupas, P. J.; Grey, C. P. *J. Catal.* **2004**, *224*, 69–79.
- (10) Chupas, P. J.; Ciraolo, M. F.; Hanson, J. C.; Grey, C. P. *J. Am. Chem. Soc.* **2001**, *123*, 1694–1702.
- (11) Chupas, P. J.; Chapman, K. W.; Kurtz, C.; Hanson, J. C.; Lee, P. L.; Grey, C. P. *J. Appl. Crystallogr.* **2008**, *41*, 822–824.
- (12) Chupas, P. J.; Chapman, K. W.; Lee, P. L. *J. Appl. Crystallogr.* **2007**, *40*, 463–470.
- (13) Paglia, G.; Buckley, C. E.; Rohl, A. L.; Hunter, B. A.; Hart, R. D.; Hanna, J. V.; Byne, L. T. *Phys. Rev. B* **2003**, *68*, 144110.
- (14) Paglia, G.; Bozin, E.; Billinge, S. J. L. *Chem. Mater.* **2006**, *18*, 3242–3248.
- (15) Page, K.; Proffen, T.; Terrones, H.; Lee, L.; Yang, Y.; Stemmer, S.; Seshadri, R.; Cheetham, A. K. *Chem. Phys. Lett.* **2004**, *393*, 385–388.
- (16) Atoji, M.; Lipscomb, W. N. *Acta Crystallogr.* **1953**, *10*, 770–774.
- (17) Chapman, K. W.; Chupas, P. J.; Kepert, C. J. *J. Am. Chem. Soc.* **2005**, *127*, 11232–11233.
- (18) Healy, M. D.; Barron, A. R. *J. Am. Chem. Soc.* **1989**, *111*, 398–399.
- (19) Leman, J. T.; Braddock-Wilking, J.; Coolong, A. J.; Barron, A. R. *Inorg. Chem.* **1993**, *32*, 4324–4336.